

Communication

Asymmetric ionic conditions generate large membrane curvatures

Marzieh Karimi, Jan Steinkuehler, Debjit Roy, Raktim Dasgupta, Reinhard Lipowsky, and Rumiana Dimova

Nano Lett., **Just Accepted Manuscript** • DOI: 10.1021/acs.nanolett.8b03584 • Publication Date (Web): 20 Nov 2018Downloaded from <http://pubs.acs.org> on November 26, 2018**Just Accepted**

“Just Accepted” manuscripts have been peer-reviewed and accepted for publication. They are posted online prior to technical editing, formatting for publication and author proofing. The American Chemical Society provides “Just Accepted” as a service to the research community to expedite the dissemination of scientific material as soon as possible after acceptance. “Just Accepted” manuscripts appear in full in PDF format accompanied by an HTML abstract. “Just Accepted” manuscripts have been fully peer reviewed, but should not be considered the official version of record. They are citable by the Digital Object Identifier (DOI®). “Just Accepted” is an optional service offered to authors. Therefore, the “Just Accepted” Web site may not include all articles that will be published in the journal. After a manuscript is technically edited and formatted, it will be removed from the “Just Accepted” Web site and published as an ASAP article. Note that technical editing may introduce minor changes to the manuscript text and/or graphics which could affect content, and all legal disclaimers and ethical guidelines that apply to the journal pertain. ACS cannot be held responsible for errors or consequences arising from the use of information contained in these “Just Accepted” manuscripts.



Asymmetric ionic conditions generate large membrane curvatures

Marzieh Karimi¹, Jan Steinkühler¹, Debjit Roy^{1,2}, Raktim Dasgupta^{1,3}, Reinhard Lipowsky¹ and Rumiana Dimova^{1*}

¹Department of Theory and Bio-Systems, Max Planck Institute of Colloids and Interfaces, Science Park Golm, 14424 Potsdam, Germany

²Present address: Department of Cell Biology and Physiology, Washington University School of Medicine, St. Louis, Missouri 63110, USA

³Laser Biomedical Applications Section, Raja Ramanna Centre for Advanced Technology, 452013 Indore, India

Abstract: Biological membranes possess intrinsic asymmetry. This asymmetry is associated not only with leaflet composition in terms of membrane species but also with differences in the cytosolic and periplasmic solutions containing macromolecules and ions. There has been a long quest for understanding the effect of ions on the physical and morphological properties of membranes. Here, we elucidate the changes in the mechanical properties of membranes exposed to asymmetric buffer conditions and the associated curvature generation. As a model system, we used giant unilamellar vesicles (GUVs) with asymmetric salt and sugar solutions on the two sides of the membrane. We aspirated the GUVs into micropipettes and attached small beads to their membranes. An optical tweezer was used to exert a local force on a bead, thereby pulling out a membrane tube from the vesicle. The assay allowed us to measure the spontaneous curvature and the bending rigidity of the bilayer in the presence of different ions and sugar. At low sugar/salt (inside/out) concentrations, the membrane spontaneous curvature generated by NaCl and KCl is close to zero, but negative in the presence of LiCl. In the latter case, the membrane bulges away from the salt solution. At high salt/sugar conditions, the membranes were observed to become more flexible and the spontaneous curvature was enhanced to even more negative values, comparable to those generated by some proteins. Our findings reveal the reshaping role of alkali chlorides on biomembranes.

Key words: spontaneous curvature, asymmetric membranes, bending rigidity, membrane nanotubes, protein-free curvature generation, giant vesicle

Introduction

Biological membranes are seldom flat but instead often exhibit strongly curved morphology. The shapes of cells and cellular organelles are highly conserved suggesting that shape and membrane morphology are crucial for life. Deformations from the molecularly preferred curvature cost significant energy, often exceeding 10 $k_B T$, and yet membrane shape transformations are ubiquitous during cellular and organelle functions. The preferred or spontaneous curvature of membranes is determined by the asymmetry across and within the bilayer^{1,2} and asymmetric conditions across the membrane is a hallmark of cellular life. However, the exact values of the spontaneous bio-membrane curvature, and how cells control this important parameter, is poorly understood. Membrane shape changes are often sustained by the action of proteins³, but this pathway is costly in terms of energy and molecular material. Ions on the other hand are abundant in the intra- and extraluminal space of cells and organelles and it is not clear whether and how they affect the membrane morphology and whether cells employ them as a cheap way of controlling membrane shape. Mammalian cells maintain ion concentration differences by a system of ion channels which enables the cell to regulate the flow of ions across the membrane. Changing sodium and potassium ion concentrations allow nerve impulses to be transmitted down a nerve cell. Ions are responsible for the maintenance of the cellular homeostasis, proper pH, osmotic pressure and water distribution in different fluid compartments of the body⁴. They are also essential for regulating the proper function of the heart and other muscles. These are some ex-

amples of important functions of sodium and potassium that make them crucial elements in cells. In addition to sodium and potassium, lithium ions (Li^+) play an important role in metabolism, neural communication, and cell proliferation⁵⁻⁶. However cellular processes controlled by lithium are not thoroughly studied, although low levels of lithium have shown beneficial effect on living organisms, e.g., lithium is a powerful drug in the treatment of manic depression⁷⁻⁸.

In conditions where the membrane is exposed to asymmetric concentration of different particles on both sides, the membrane prefers to bulge toward one of the aqueous compartments. This response results from molecular interactions, i.e., either adsorption or depletion. These interactions may have different effects on the bilayer structure. An adsorbed ion or solute, for example, may insert into the leaflet and push the lipids apart, thereby increasing the effective molecular area. Alternatively, an adsorbed specie could also lead to local condensation of lipids, thereby reducing the effective molecular area. This behavior is described by the spontaneous (preferred) curvature of the membrane. It can be positive or negative if the membrane bends away from or towards the lumen, respectively^{1,9}. There have been a long quest to understand the effect of ions on the physical and morphological properties of the membrane. Considering the strong ion-lipid interactions supported by abundant evidence for adsorption of ions to the membrane (see e.g. ¹⁰ and references therein) and, in particular, the recent findings on the impact of ion trans-membrane asymmetry on the membrane phase state¹¹, we set to investigate the effect of ion asymmetry on the mechanical properties

of the membranes. We used giant unilamellar vesicles (GUVs) as a model membrane system¹²⁻¹⁴. Their large size (in the range of tens of microns) enable us to manipulate the vesicle membranes and visualize the membrane response using optical microscopy. We aimed at investigating and quantifying the effect of Na⁺, K⁺, and Li⁺ and their transmembrane asymmetry on the mechanical properties of phosphatidylcholine (POPC) model membranes.

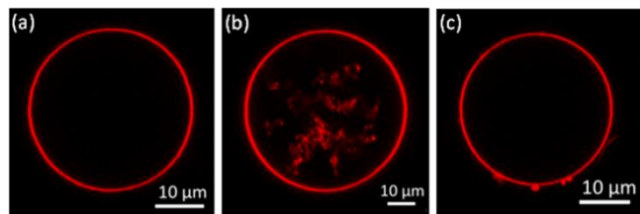


Figure 1. Confocal cross sections of different POPC GUVs with their two leaflets exposed to different solutions of sucrose and salts. GUVs were fluorescently labeled with 0.1 mol% Texas-Red-DHPE and classified as either (a) exhibiting no structures, (b) containing numerous nanotubes inside the vesicle, or (c) exhibiting structures (small buds, tubes, folds or even adhering vesicles) pointing to the outside. Depending on the concentration difference of the salts on the two sides of the membrane, the relative frequency of each morphology changed. The results are summarized in Table 1.

Experimental Section

Vesicle preparation. GUVs were prepared using the electroformation technique from 2 mM of POPC and 0.1-0.2 mol% of 1,2-dioleoyl-*sn*-glycero-3-phosphoethanolamine-*N*-(cap biotinyl). Additionally, 0.1 mol% Texas Red 1,2-dihexadecanoyl-*sn*-glycero-3-phosphoethanolamine (Texas-Red-DHPE) was added for fluorescence imaging of the vesicles, see Section S1 in the SI.

Experimental setup. The tube-pulling setup is a combination of the micromanipulation and optical tweezers¹⁵⁻¹⁶. Micromanipulation was performed using micropipettes of ~7 μm inner diameters for the aspiration and setting the membrane tension of GUVs (section S2 in SI). The optical tweezers setup¹⁶ was calibrated by application of known hydrodynamic forces on the beads and subsequent imaging of the bead position in the trap, see Section S3 in SI). This calibration was later used to estimate the forces when the bead is displaced from the trap center by the pulled nanotube. Curve fitting and data analysis was performed using image analysis implemented in MATLAB 2018b¹⁵ and Origin 2018.

Results and Discussion

We prepared GUVs composed of POPC doped with fluorescent lipid by electroformation as described in the Methods section and Section S1 in the Supporting Information (SI). The vesicles were grown in sugar solutions, which were in this way encapsulated in the GUVs. Subsequent 1:20 dilution of the GUVs in slightly hypotonic salt solutions allowed the study of sugar-salt solution asymmetry on the lipid membrane (the inverse condition of salt inside and sugar outside was not feasible as no suitable vesicles could be produced for the explored salt concentrations). The GUV morphologies in asymmetric solution conditions were imaged with confocal microscopy. In solutions of rather low salt concentrations up to approximately 30 mM of NaCl, the GUVs exhibited mostly smooth, nearly spherical, membranes (Fig. 1a, Table 1, condi-

tion a). Such vesicle morphologies indicate negligible membrane spontaneous curvature and are typical for GUVs in nearly symmetric solution conditions (data not shown). Strikingly, LiCl solution of similar concentration results in GUVs with highly curved membrane segments (nanotubes) pointing to the vesicle interior with diameters below the optical resolution (Figure 1b, Table 1, condition e). Direct observations of individual vesicles upon solution exchange showed the formation of the tubes induced by LiCl asymmetry, see Fig. S1 in the SI. They were reminiscent of cylindrical and necklace-like tubes observed in studies with membranes exposed to polymer asymmetry¹⁷⁻¹⁸. Increasing NaCl and KCl concentrations up to physiological levels (150 mM) lead to a similar tendency for inward pointing nanotubes (Table 1, conditions b, c and d); note that the fraction of external structures also increases which results not only from outward membrane protrusions but also adhesion of smaller vesicles. In principle, optical observation of tubes or buds allows for direct quantification of the membrane spontaneous curvature^{2, 18-19}. However, adhesion of small vesicles to the GUVs (Fig. 1c, which would be counted as external structures in Table 1), most prominent at high NaCl concentrations, interferes with clear assessment of the spontaneous curvature from such morphological studies alone. High LiCl were not investigated due to the strong adhesion of GUVs to each other.

To quantify the spontaneous curvature, we applied the more quantitative method of pulling of membrane nanotubes from the GUV membrane, see e.g.^{15, 20}. In this method, GUVs are aspirated with a micropipette, which controls the membrane tension Σ_{asp} of the vesicles by changing the hydrostatic pressure difference applied by changing the height of a water reservoir connected to the pipette, see Section S2 in the SI. A 2 μm streptavidin bead trapped by optical tweezers was stuck to the vesicle and used to pull a membrane nanotube with 10 μm length from the GUV. In this configuration, the pulling force can be estimated from the position of the bead in the optical trap which was measured by optical microscopy, see Section S3 in the SI. The pulling force f for an outward tube is given by^{1, 15}:

$$f = 2\pi\sqrt{2\kappa\Sigma_{asp}} - 4\pi\kappa m \quad (1)$$

where κ is the bending rigidity and m is the membrane spontaneous curvature. Thus, by measuring the force for different membrane tension set by the pipette, one can deduce the bending rigidity from the slope of the data (first term in Eq. 1) and the spontaneous curvature from the intercept (second term). Figure 2 represents the experiment schematic and images of vesicles with a pulled membrane nanotube.

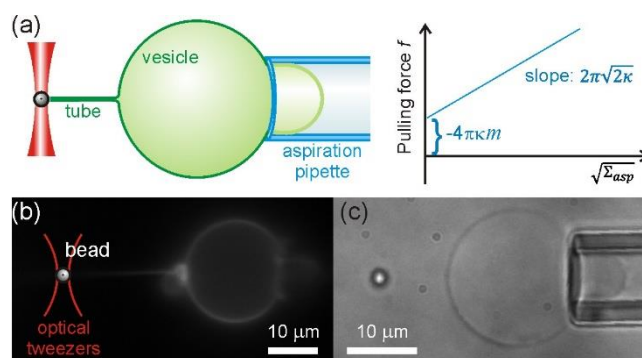


Figure 2. Experimental assay for pulling out a nanotube from a GUV: (a) sketch of the setup and principle of measurement, and

(b) epifluorescence and (c) bright-field images of an aspirated vesicle with a pulled tube.

Table 1. Statistics of internal and external structures, compare Fig. 1, for GUVs exposed to different solutions of sucrose and salt: (a) GUVs were grown in 54 mM sucrose (inside) and diluted to 28.5 mM NaCl and 2.7 mM sucrose (outside); the total number of vesicles studied for this asymmetry was $n = 50$. (b) GUVs with 260 mM sucrose inside, and 142.5 mM NaCl plus 13 mM sucrose outside; $n = 130$. (c) GUVs with 114 mM sucrose inside, and 57 mM KCl plus 5.7 mM sucrose outside; $n = 58$. (d) GUVs with 260 mM sucrose inside, and 142.5 mM KCl plus 13 mM sucrose outside; $n = 135$. (e) GUVs with 54 mM sucrose inside, and 28.5 mM LiCl plus 2.7 mM sucrose outside; $n = 85$. The given fractions have an uncertainty of about 15%. The observed external structures include small buds and tubes, but also adhering vesicles.

Asymmetry conditions		No structures	Internal structures	External structures
a	Low NaCl	82 %	6 %	2 %
b	High NaCl	29 %	30 %	41 %
c	Low KCl	34 %	39 %	27 %
d	High KCl	6 %	77 %	17 %
e	Low LiCl	20 %	69 %	10 %

The streptavidin-coated beads were injected into the experimental chamber locally via a syringe and were moved into the proximity of a GUV using the optical tweezers (see Material and Methods and Section S2). A freely fluctuating GUV was aspirated into the glass capillary, a bead stuck to it and a nanotube was pulled out by translating the vesicle away. Tube pulling experiments started with low concentration of NaCl outside the membrane, which was identified as the minimal salt concentration where bead-membrane adhesion was still efficient. As determined in the morphological studies of GUVs, this concentration was used further as a reference to compare our data to conditions that induce higher membrane asymmetry. Note that controls with symmetric sugar conditions were not possible as beads were not adhering to the membrane and thus tubes could not be pulled in the absence of salt. In all experimental conditions, vesicles were studied at suction pressures between ~ 20 Pa and ~ 49 Pa. The membrane tension of the vesicles at each pressure could be assessed from the geometry of the aspirated vesicle and the applied pressure difference, see SI Section S2. By careful calibration of the optical trap, the force exerted on the bead holding the nanotubes was determined from the optically measured bead displacement (see Material and Methods and SI Sections S3 and S4). When measuring tube pulling forces, the trapped bead was displaced to the edge of the trap, i.e. away from the linear region of the trapping force field. This allowed us, for the same trap beam power, to measure higher forces than when using the linear trapping force region. This is an advantageous approach as in this way the heating of the bead and the attached membrane is reduced²¹⁻²². Moreover, considering possible variations of sizes of the trapped latex beads we calibrated the trap stiffness for each individual bead before using it for pulling tubes. An approach combining the equipartition method and viscous drag method was used (see SI Section S4).

By fitting all force vs. tension data points to a linear fit following Eq. 1, the mean bending rigidity of vesicles with low NaCl

asymmetry (Fig. 3a) was estimated as $(34.79 \pm 0.81)k_B T$. This value is well within the range of data reported for POPC membranes²³ and in particular for POPC vesicles in the presence of NaCl as measured from fluctuation analysis²⁴⁻²⁵. The spontaneous curvature of the membrane determined from the y-axis intercept of the fitted line was found to be $(0.66 \pm 0.30) \mu\text{m}^{-1}$; note that fitting individual measurements and subsequent averaging yields $(0.09 \pm 0.68) \mu\text{m}^{-1}$, see Table S1. This spontaneous curvature is negligible (comparable to the mean curvature of the GUVs) which is consistent with the spherical nontubulated morphologies observed in the microscopy images statistics (Table 1).

Identical experiments were performed on vesicles exposed to high asymmetry of physiological concentration (150 mM) of NaCl outside and isotonic sucrose inside the vesicles. Six vesicles were studied in this condition and the mean bending rigidity was estimated to be $(23.60 \pm 0.60)k_B T$ (Fig. 3a). Comparing the bending rigidity in the two explored NaCl conditions, we conclude that the bending rigidity decreases by increasing NaCl (and sugar) concentration, confirming a trend reported in Refs.²⁴⁻²⁵ (note that salts are reported to rigidify bilayer stacks, see e.g.²⁶, which underlies the difference in the behavior of single membranes as in giant vesicles and multiple layers as in multilayered systems, each exploring lipid-to-ion ratios which differ by orders of magnitude). As a reminder, at high salt asymmetry, the sugar concentration inside the vesicles is also increased and sugars have been also shown to decrease the membrane bending rigidity (see overview in²³) presumably because of membrane thinning in this concentration range²⁷. It can be also seen from Fig. 3a that while the intercept of the linear fit under low asymmetry is zero within the fitting accuracy (blue shaded region), the intercept at high NaCl asymmetry implies non-zero spontaneous curvature. We estimated this negative spontaneous curvature as $-(8.74 \pm 0.50) \mu\text{m}^{-1}$, again consistent with the spontaneous appearance of membrane tubes with diameters below optical resolution ($< 0.5 \mu\text{m}$) observed in the morphology studies (Table 1). The values obtained for the spontaneous curvature imply that it would stabilize cylindrical tubes with diameter around 110 nm. Measuring the tube diameter using fluorescence intensity as done in Refs.²⁸⁻²⁹ was not feasible as our microscope setup was equipped for epifluorescence only where bleaching poses a problem.

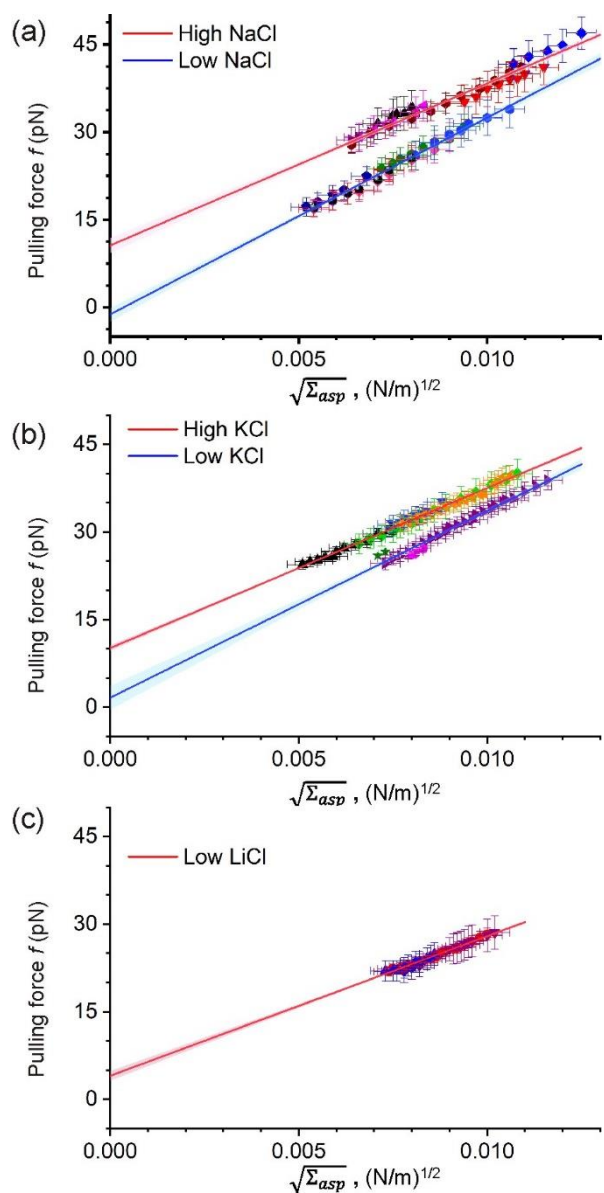


Figure 3. Results for out tubes showing the pulling force (f) vs. the square root of the membrane tension Σ_{asp} for vesicles exposed to low asymmetry (blue linear fits) and high asymmetry (red linear fits) of sucrose inside and (a) NaCl outside, (b) KCl outside and (c) LiCl outside the vesicles (the respective solution concentrations are given in the caption of Table 1). Differently colored symbols reflect measurements on different vesicles from different preparations. The solid lines are fits following Eq. 1 yielding the material properties of the membrane, i.e., the bending rigidity and spontaneous curvature as schematically illustrated in Fig. 2a.

In some of the experiments at high NaCl asymmetry, the measured spontaneous curvature was found close to zero, but upon inspection of the vesicle population with phase contrast microscopy and employing encapsulated water-soluble fluorophore, we found that this is because vesicles have leaked and the asymmetry has been compromised, see SI Section S5.

Table 2. Mean values and standard deviations of the bending rigidity and the spontaneous curvature of vesicle membranes exposed to asymmetric solutions of sucrose and salt as described in the caption of Table 1. Each value is obtained from a fit to all data for a given buffer composition. For values obtained from individual fits and subsequent averaging, see Section S6 and

Tables S1-S5 in the SI. The exact salt and sugar concentration conditions are given in Table 1.

Condition	$\kappa(k_B T)$	$m(\mu\text{m}^{-1})$
Low NaCl	34.79 ± 0.81	0.66 ± 0.30
High NaCl	23.60 ± 0.60	-8.74 ± 0.50
Low KCl	31.87 ± 1.08	-1.00 ± 0.59
High KCl	23.11 ± 0.24	-8.47 ± 0.24
Low LiCl	17.52 ± 0.34	-4.45 ± 0.45

Similar experiments were performed for asymmetric KCl solutions. Concentration-wise, the low-asymmetry condition here do not correspond to that of low NaCl asymmetry as higher concentration of KCl were required to ensure the beads sticking to the membrane. The respective bending rigidity values were $(31.87 \pm 1.08)k_B T$ and $(23.11 \pm 0.24)k_B T$ for low and high asymmetries indicating softening of the membrane by KCl as observed for NaCl. Similarly, increasing KCl asymmetry was found to induce significant negative spontaneous curvature on the membranes, see Fig. 3b and data summarized in Table 2. To recapture, the bending rigidity and spontaneous curvature values are comparable for vesicles exposed to two different salts i.e. NaCl and KCl in two different concentration ranges, i.e. each of these alkali chlorides affects the membrane similarly in terms of softening and curvature generation.

Finally, we also explored the effect of LiCl asymmetry. Even though physiological concentrations of lithium are in the (sub)millimolar range, studies on axonal remodeling and growth cone spreading (see e.g.³⁰) explore concentrations on the order of 10 mM. To compare our results on NaCl asymmetry, we explored LiCl asymmetry at the same ion concentration, see Fig. 3c and Table 1 for exact conditions. Even at this low LiCl concentration the bending rigidity is considerably decreased and a significant negative spontaneous curvature was measured consistent with microscopy observations (Table 1). All experiments are summarized in Table 2.

To confirm the effect of the salts on the lipid bilayers, the membrane bending rigidity was also measured via fluctuation analysis³¹, see Section S7 in the SI. The values of bending rigidity were estimated to be $(29.8 \pm 3.7)k_B T$ and $(19.2 \pm 5.0)k_B T$ for vesicles exposed to low asymmetry of KCl and LiCl, respectively. These results are in good agreement with the bending rigidity values obtained from tube pulling experiments in Table 2.

Conclusions

In this paper, we used a combination of optical tweezers and micropipette manipulation of giant vesicles to pull out lipid nanotubes and measure fundamental mechanical properties of the membranes. We focused on the effect of ionic asymmetry across the membrane as present in cells. The vesicles were exposed to different concentrations of sucrose (inside) and three different types of salts (outside), namely NaCl, KCl and LiCl. Measurements of the tube pulling force and membrane tension of the vesicles, allowed us to assess the bending rigidity and spontaneous curvatures generated in the above conditions. The magnitude for the spontaneous curvature generated at high NaCl and KCl asymmetry is lower than values measured on membranes exposed to BAR domain proteins³² ($m^{-1} \sim 20 \div 100 \text{ nm}$) and comparable to that of membranes with asymmetric distribution of gangliosides^{15, 33}, polymers¹⁸ and more importantly divalent ions³⁴⁻³⁵ ($m^{-1} \sim 100 \div 500$

nm). The sign of the spontaneous curvature generated by calcium reported in Refs.³⁴⁻³⁵ is controversial - one group reported that binding of calcium ions to these membranes generates positive spontaneous curvature³⁴, whereas measurements of another group at the same conditions yielded negative spontaneous curvature³⁵. Our results for NaCl and KCl corroborate negative spontaneous curvature at high salt concentration. Indeed, similarly to direct calcium-induced inward tubulation shown in³⁶ we do observe more abundant internal tubes in these vesicles (Table 1). Thus, in the presence of salt solutions, vesicle membranes tend to curve away from the exterior salt solution attaining a negative spontaneous curvature. Presumably, the adsorbed ions lead to local condensation of lipids, thereby reducing the effective molecular area of the leaflet exposed to them.

Interestingly, increasing salt asymmetries correlated with the change in the values of both the bending rigidity and spontaneous curvature. Generally, sugars are thought to soften membranes via thinning of the bilayers²⁷ while alkali ions, except for lithium, are considered as not interacting with the membrane³⁷. As suggested by simulations and NMR data³⁷, we thus speculate that the spontaneous curvature is generated by sodium and potassium ions depletion from the bilayer (outer leaflet) while the adsorbed lithium (similarly to the effect of calcium) leads to local condensation of lipids, thereby reducing the effective molecular area of the leaflet exposed to them. From fluorescence lifetime measurements³⁸ we attempted to distinguish the condensing effect of lithium ions from the depletion of sodium and potassium ions from the membrane, see Section S8 in the SI. The lifetime of the used dye was altered only in the presence of LiCl (corresponding to the low LiCl asymmetry condition explored here) but not in the presence of NaCl and KCl solutions (both in high and low asymmetry conditions). We thus conclude that our speculations for the depletion of sodium and potassium ions from the membrane as well as for the condensing effect of lithium are reasonable. Presumably, molecular dynamics simulation studies will be able to further characterize the mechanism of curvature generation by monovalent salt asymmetry. In our experiments, the effect of the ions may be also enhanced by thinning of the monolayer facing the sugar solution (sugars are believed to laterally expand the leaflet²⁷), all together driving the generation of the negative spontaneous curvature. One significant result to be emphasized here is that the bending rigidity and negative curvature generated by both NaCl and KCl are comparable. While, the vesicle membrane has almost zero spontaneous curvature at low concentration of these salts, low concentration of LiCl induces a negative curvature which is approximately equivalent to half the value measured for the high asymmetry conditions with NaCl and KCl. In a number of studies, lithium has been shown to have an inhibitory role on proteins (see e.g.^{8, 30, 39} and references therein) leading to the conclusion that neuronal remodeling is predominantly governed by the activity of these proteins. Here, we show that biomembrane reshaping might result not solely from protein inhibition by lithium but also by the direct action of LiCl on membrane rigidity and spontaneous curvature resulting from the applied asymmetric solutions.

Acknowledgements

This work is part of the MaxSynBio consortium which was jointly funded by the Federal Ministry of Education and Research of Germany and the Max Planck Society.

Supporting Information

Vesicles preparation and observation; micropipette manipulation and optical trapping and calibration; bending rigidity and spontaneous curvature data from individual vesicles; fluctuation analysis; fluorescence lifetime measurements.

Conflict of Interest Disclosure

The authors declare no conflict of interest.

AUTHOR INFORMATION

Corresponding Author

Rumiana Dimova: dimova@mpikg.mpg.de

ORCID IDs

Marzieh Karimi: [0000-0002-0984-0730](https://orcid.org/0000-0002-0984-0730)

Jan Steinkühler: [0000-0003-4226-7945](https://orcid.org/0000-0003-4226-7945)

Debjit Roy: [0000-0001-8986-9359](https://orcid.org/0000-0001-8986-9359)

Raktim Dasgupta: [0000-0003-1423-1937](https://orcid.org/0000-0003-1423-1937)

Reinhard Lipowsky: [0000-0001-8417-8567](https://orcid.org/0000-0001-8417-8567)

Rumiana Dimova: [0000-0002-3872-8502](https://orcid.org/0000-0002-3872-8502)

Author Contributions

RD, JS and MK designed the experiments. MK and JS performed the experiments. RD, DR, JK, MK and RD developed the trap calibration assay. All authors wrote the manuscript.

REFERENCES

1. Lipowsky, R., Spontaneous tubulation of membranes and vesicles reveals membrane tension generated by spontaneous curvature. *Faraday Discuss.* **2013**, *161*, 305-331.
2. Bassereau, P.; Jin, R.; Baumgart, T.; Deserno, M.; Dimova, R.; Frolov, V. A.; Bashkirov, P. V.; Grubmüller, H.; Jahn, R.; Risselada, H. J.; Johannes, L.; Kozlov, M. M.; Lipowsky, R.; Pucadyil, T. J.; Zeno, W. F.; Stachowiak, J. C.; Stamou, D.; Breuer, A.; Lauritsen, L.; Simon, C.; Sykes, C.; Voth, G. A.; Weikl, T. R., The 2018 biomembrane curvature and remodeling roadmap. *J. Phys. D: Appl. Phys.* **2018**, *51* (34), 343001.
3. Zimmerberg, J.; Kozlov, M. M., How proteins produce cellular membrane curvature. *Nat. Rev. Mol. Cell Biol.* **2005**, *7*, 9.
4. Pohl, H. R.; Wheeler, J. S.; Murray, H. E., Sodium and Potassium in Health and Disease. In *Interrelations between Essential Metal Ions and Human Diseases*, Sigel, A.; Sigel, H.; Sigel, R. K. O., Eds. Springer Netherlands: Dordrecht, 2013; pp 29-47.
5. Shahzad, B.; Mughal, M. N.; Tanveer, M.; Gupta, D.; Abbas, G., Is lithium biologically an important or toxic element to living organisms? An overview. *Environmental Science and Pollution Research* **2017**, *24* (1), 103-115.
6. Williams, R.; Ryves, W. J.; Dalton, E. C.; Eickholt, B.; Shaltiel, G.; Agam, G.; Harwood, A. J., A molecular cell biology of lithium. *Biochem. Soc. Trans.* **2004**, *32*, 799-802.
7. Pasternak, C. A., *Monovalent cations in biological systems*. CRC press: 1990.
8. Klein, P. S.; Melton, D. A., A molecular mechanism for the effect of lithium on development. *Proceedings of the National Academy of Sciences* **1996**, *93* (16), 8455.
9. Lipowsky, R., Coupling of bending and stretching deformations in vesicle membranes. *Adv. Colloid Interface Sci.* **2014**, *208*, 14-24.

10. Klasczyk, B.; Knecht, V.; Lipowsky, R.; Dimova, R., Interactions of Alkali Metal Chlorides with Phosphatidylcholine Vesicles. *Langmuir* **2010**, *26* (24), 18951-18958.
11. Kubsch, B.; Robinson, T.; Lipowsky, R.; Dimova, R., Solution Asymmetry and Salt Expand Fluid-Fluid Coexistence Regions of Charged Membranes. *Biophys. J.* **2016**, *110* (12), 2581-2584.
12. Dimova, R.; Aranda, S.; Bezlyepkina, N.; Nikolov, V.; Riske, K. A.; Lipowsky, R., A practical guide to giant vesicles. Probing the membrane nanoregime via optical microscopy. *J. Phys.: Condens. Matter* **2006**, *18* (28), S1151-S1176.
13. Walde, P.; Cosentino, K.; Engel, H.; Stano, P., Giant Vesicles: Preparations and Applications. *ChemBioChem* **2010**, *11* (7), 848-865.
14. Dimova, R., Giant Vesicles: A Biomimetic Tool for Membrane Characterization. In *Advances in Planar Lipid Bilayers and Liposomes*, Iglič, A., Ed. Academic Press: 2012; Vol. Volume 16, pp 1-50.
15. Dasgupta, R.; Miettinen, M. S.; Fricke, N.; Lipowsky, R.; Dimova, R., The glycolipid GM1 reshapes asymmetric biomembranes and giant vesicles by curvature generation. *Proc. Natl. Acad. Sci. U. S. A.* **2018**, *115*, 5756-5761.
16. Kraikivski, P.; Pouligny, B.; Dimova, R., Implementing both short- and long-working-distance optical trappings into a commercial microscope. *Rev. Sci. Instrum.* **2006**, *77* (11), 113703.
17. Li, Y.; Lipowsky, R.; Dimova, R., Membrane nanotubes induced by aqueous phase separation and stabilized by spontaneous curvature. *Proc. Natl. Acad. Sci. U. S. A.* **2011**, *108* (12), 4731-4736.
18. Liu, Y.; Agudo-Canalejo, J.; Grafmüller, A.; Dimova, R.; Lipowsky, R., Patterns of Flexible Nanotubes Formed by Liquid-Ordered and Liquid-Disordered Membranes. *ACS Nano* **2016**, *10* (1), 463-474.
19. Nikolov, V.; Lipowsky, R.; Dimova, R., Behavior of giant vesicles with anchored DNA molecules. *Biophys. J.* **2007**, *92* (12), 4356-4368.
20. Sorre, B.; Callan-Jones, A.; Manneville, J. B.; Nassoy, P.; Joanny, J. F.; Prost, J.; Goud, B.; Bassereau, P., Curvature-driven lipid sorting needs proximity to a demixing point and is aided by proteins. *Proc. Natl. Acad. Sci. U. S. A.* **2009**, *106* (14), 5622-5626.
21. Liu, Y.; Cheng, D. K.; Sonek, G. J.; Berns, M. W.; Chapman, C. F.; Tromberg, B. J., Evidence for localized cell heating induced by infrared optical tweezers. *Biophys. J.* **1995**, *68* (5), 2137-2144.
22. Bolognesi, G.; Friddin, M. S.; Salehi-Reyhani, A.; Barlow, N. E.; Brooks, N. J.; Ces, O.; Elani, Y., Sculpting and fusing biomimetic vesicle networks using optical tweezers. *Nature Communications* **2018**, *9* (1), 1882.
23. Dimova, R., Recent developments in the field of bending rigidity measurements on membranes. *Adv. Colloid Interface Sci.* **2014**, *208* (0), 225-234.
24. Bouvrais, H. Mechanical properties of giant vesicle membranes investigated by flickering technique. PhD thesis, University of Southern Denmark, Odense, 2011.
25. Bouvrais, H., Bending Rigidities of Lipid Bilayers: Their Determination and Main Inputs in Biophysical Studies. In *Advances in Planar Lipid Bilayers and Liposomes*, Iglič, A., Ed. Academic Press: 2012; Vol. Volume 15, pp 1-75.
26. Pabst, G.; Hodzic, A.; Strancar, J.; Danner, S.; Rappolt, M.; Laggner, P., Rigidification of neutral lipid bilayers in the presence of salts. *Biophys. J.* **2007**, *93* (8), 2688-2696.
27. Andersen, H. D.; Wang, C. H.; Arleth, L.; Peters, G. H.; Westh, P., Reconciliation of opposing views on membrane-sugar interactions. *Proc. Natl. Acad. Sci. U. S. A.* **2011**, *108* (5), 1874-1878.
28. Sorre, B.; Callan-Jones, A.; Manzi, J.; Goud, B.; Prost, J.; Bassereau, P.; Roux, A., Nature of curvature coupling of amphiphysin with membranes depends on its bound density. *Proc. Natl. Acad. Sci. U. S. A.* **2012**, *109* (1), 173-178.
29. Aimon, S.; Callan-Jones, A.; Berthaud, A.; Pinot, M.; Toombes, Gilman E. S.; Bassereau, P., Membrane Shape Modulates Transmembrane Protein Distribution. *Dev. Cell* **2014**, *28* (2), 212-218.
30. Hall, A. C.; Lucas, F. R.; Salinas, P. C., Axonal Remodeling and Synaptic Differentiation in the Cerebellum Is Regulated by WNT-7a Signaling. *Cell* **2000**, *100* (5), 525-535.
31. Gracià, R. S.; Bezlyepkina, N.; Knorr, R. L.; Lipowsky, R.; Dimova, R., Effect of cholesterol on the rigidity of saturated and unsaturated membranes: fluctuation and electrodeformation analysis of giant vesicles. *Soft Matter* **2010**, *6* (7), 1472-1482.
32. McMahon, H. T.; Gallop, J. L., Membrane curvature and mechanisms of dynamic cell membrane remodelling. *Nature* **2005**, *438* (7068), 590-596.
33. Bhatia, T.; Agudo-Canalejo, J.; Dimova, R.; Lipowsky, R., Membrane Nanotubes Increase the Robustness of Giant Vesicles. *ACS Nano* **2018**, *12* (5), 4478-4485.
34. Simunovic, M.; Lee, K. Y. C.; Bassereau, P., Celebrating Soft Matter's 10th anniversary: screening of the calcium-induced spontaneous curvature of lipid membranes. *Soft Matter* **2015**, *11* (25), 5030-5036.
35. Graber, Z. T.; Shi, Z.; Baumgart, T., Cations induce shape remodeling of negatively charged phospholipid membranes. *Phys. Chem. Chem. Phys.* **2017**, *19* (23), 15285-15295.
36. Ali Doosti, B.; Pezeshkian, W.; Bruhn, D. S.; Ipsen, J. H.; Khandelia, H.; Jeffries, G. D. M.; Lobovkina, T., Membrane Tubulation in Lipid Vesicles Triggered by the Local Application of Calcium Ions. *Langmuir* **2017**, *33* (41), 11010-11017.
37. Catte, A.; Girysh, M.; Javanainen, M.; Loison, C.; Melcr, J.; Miettinen, M. S.; Monticelli, L.; Määttä, J.; Oganessian, V. S.; Ollila, O. H. S.; Tynkkynen, J.; Vilov, S., Molecular electrometer and binding of cations to phospholipid bilayers. *Phys. Chem. Chem. Phys.* **2016**, *18* (47), 32560-32569.
38. Packard, B. S.; Wolf, D. E., Fluorescence lifetimes of carbocyanine lipid analogs in phospholipid bilayers. *Biochemistry* **1985**, *24* (19), 5176-5181.
39. Williams, R. S. B.; Cheng, L.; Mudge, A. W.; Harwood, A. J., A common mechanism of action for three mood-stabilizing drugs. *Nature* **2002**, *417*, 292.

for TOC only

